A novel Hamilton receptor monomer for the stoichiometric molecular imprinting of barbiturates

Stefania Lettieri[a1], Panagiotis Manesiotis[b], Molly Slann[c], Dewi W. Lewis[c] and Andrew J. Hall[a*]

[a] Medway School of Pharmacy, Universities of Greenwich & Kent at Medway, Central Avenue, Chatham, Chatham Maritime, Kent, United Kingdom ME4 4TB.

[b] School of Chemistry and Chemical Engineering, David Keir Building, Stranmillis Road, Belfast, Northern Ireland BT9 5AG.

[c] Department of Chemistry, University College London, 20 Gordon Street, London WC1H 0AJ.

[1] Present address: Italian Institute for Technology, via Livorno 60, 10144 Torino, Italy.

Corresponding author: Andrew J. Hall

Tel: +44 (0)1634 202952 | **Fax:** +44 (0)1634 883927 | **E-mail:** A.Hall@kent.ac.uk

Authors: Stefania Lettieri[a1] StefaniaLettieri@iit.it

Panagiotis Manesiotis[b] p.manesiotis@qub.ac.uk

Molly Slann[c] molly.slann.16@ucl.ac.uk

Dewi W. Lewis[c] d.w.lewis@ucl.ac.uk

Abstract

New molecularly imprinted polymers (MIPs) for the recognition of barbiturates were synthesised by “bulk” polymerisation. These polymers were prepared using pentobarbital as the template in combination with a novel Hamilton receptor functional monomer. The solution binding properties of the monomer were assessed by NMR titration experiments, showing high affinity for barbiturates and lower affinity for related compounds lacking the ability to form as many hydrogen bonds. The properties of the MIP were assessed via equilibrium rebinding experiments and in the chromatographic mode, and compared to the behaviour of a control non-imprinted polymer (NIP). The MIP showed a far higher population of binding sites with higher affinity than the NIP which was reflected in the chromatographic evaluation, where the template and a related barbiturate were not eluted from the MIP within 60 minutes, while their retention was weak on the NIP, leading to extremely high imprinting factors. Other analytes were weakly retained by MIP and NIP, with those presented an acceptor-donor-acceptor array of hydrogen bonding sites most retained. Preliminary molecular modelling studies support the hypothesis that the presence of the template in the MIP synthesis “chooses” the conformation of the functional monomer that is “locked in” during the polymerisation.

Keywords: molecularly imprinted polymer, barbiturates, Hamilton receptor

1. Introduction

The barbiturates are a class of drugs with hypnotic, sedative and anxiolytic effects. First discovered in the early 20th century, they were introduced to the clinic in 1904. Their use started to decline in the 1960s, due to the growing acceptance that they led to dependency and a growing number of deaths linked to their use [1]. Though now largely supplanted by the preferred use of benzodiazepines, barbiturates still find uses in the treatment of insomnia, epilepsy and as an inducer of general anaesthesia [2-4]. Barbiturate poisoning has led to between 28 and 50 deaths annually in the UK since 2012 [5].

Molecular imprinting is a templated polymer synthesis which leads to synthetic receptors (molecularly imprinted polymers, MIPs) capable of recognising the template structure and / or analogous structures with high fidelity [6]. This occurs through the creation of specific binding cavities during the polymerisation process, these cavities being complementary to the chosen template in terms of shape, size and functionality. The most common approach is the so-called non-covalent method, whereby template and (functional) monomers are envisaged to form complexes via non-covalent interactions which are then locked in place through copolymerisation with a cross-linking monomer. Post-polymerisation extraction of the template reveals the imprinted binding cavities. MIPs have been created for templates across a wide range of length scales, from small molecule drugs [7] and herbicides [8], through peptides [9], to biological macromolecules [10], viruses [11] and even whole cells [12]. MIPs have been applied in analytical procedures, such as solid phase extraction (SPE) [13] and biomimetic sensors [14]. More recently, their use in bioimaging and therapy have been increasingly explored [15,16].

The overwhelming majority of non-covalent MIPs are prepared using commercially available functional monomers that are generally capable of only weak to moderate interactions with any given template. They are thus used in excess, leading to monomer residues not associated with template being scattered throughout the polymer structure. This is believed to be a major source of non-selective binding by such MIPs. An alternative is to use monomers designed to recognise a particular functionality or molecule, e.g. the use of amidine-based monomers by the groups of Wulff [17] and Haupt [18] or urea-based monomers by Sellergren *et al*. [19] to recognise oxyanion functionality. The use of these monomers in stoichiometric non-covalent imprinting has opened to door a variety of exciting applications in disease

biomarker enrichment [20] and, more recently, towards MIP-based therapeutics [21]. A more complex example of this strategy is highlighted by the work of Turner *et al.* [22] in their use of functionalised aptamers as functional monomers in imprinting protocols. The major benefits of designing specific functional monomers are the increased yields of high affinity, selective binding sites and the reduced levels of non-specific binding observed. Such a strategy also allows the incorporation of signal transduction elements alongside the enhanced binding, e.g. fluorescence-active MIPs [23].

MIPs selective for barbiturates may find use in a number of different applications: (1) as part of a sensor system for monitoring levels in patient plasma or urine [24]; (2) in solid phase extraction for sample clean-up and enrichment of patient samples prior to analysis, avoiding complications due to sample complexity arising from concomitant use of a range of drug substances [25]; (3) as a putative therapeutic for the capture and removal of barbiturates from a patient's bloodstream following poisoning [26].

The imprinting of barbiturates has been reported previously, the most successful examples being those reported by Takeuchi *et al*. [27, 28], who used 2,6-bis(acrylamido)pyridine as functional monomer in a stoichiometric manner*, i.e.* two monomer units per template. This work was inspired by the earlier work of Hamilton *et al*. [29, 30], who created a series of artificial receptors for barbiturates. These receptors contained a hydrogen bonding core containing two 2,6-diaminopyridine units linked through different spacers and were shown to bind to barbiturates with affinities in the range of $10^5 – 10^6$ M^{-1} in chloroform.

We decided to revisit these Hamilton cleft structures and here present our results on the synthesis of a novel Hamilton cleft-like functional monomer and its solution binding properties. Thereafter we present the preparation and performance of the MIP prepared using this monomer in comparison to a control non-imprinted polymer (NIP).

2. Experimental

2.1 Materials and physicochemical characterisation

All solvents and reagents were used without purification with the exception of ethylene glycol dimethacrylate (EGDMA), which was freed from inhibitor and purified before use as follows: EGDMA was washed sequentially with 10 % aqueous NaOH and brine, then dried over $MgSO_4$. After filtration, EGDMA was distilled under reduced pressure and stored at -20°C prior to use. 5-t*ert*-butylisophthalic acid, 5-methyluridine (5-MeU)

and uracil were purchased from Tokyo Chemical Industries (TCI) (Oxford, UK). Pseudouridine (ψ), uridine, 2',3',4'-tri-*O*-acetyluridine (TAU), pentobarbital and phenobarbital were purchased from Carbosynth (Compton, UK). Deuterated chloroform and dimethyl sulfoxide (DMSO) were purchased from Goss Scientific (Crewe, UK). Azo-*bis*-dimethylvaleronitrile (ABDV) was received from DuPont BV (Netherlands). All the other analytes, reagents and solvents were purchased from Sigma Aldrich (Gillingham, UK). 2′,3′,4′-tri-*O*-propionyl uridine (TPU), 2′,3′,4′-tri-*O*-butyryl uridine (TBU) and 2',3',4'-tri-*O*-acetylpseudouridine (TAψ) were prepared from Uridine or pseudouridine and the appropriate acid anhydride using a literature method [31] and their synthesis has been reported previously [32]. Thin-layer chromatography (TLC) was performed on aluminium-backed plates MERCK silica gel 60 F254 (Fluka Analytics).

Melting points were determined using a STUART melting point apparatus and are uncorrected. Infrared spectra were recorded on a Perkin Elmer Spectrum One FT-IR Spectrometer. ^{1}H NMR and ^{13}C NMR spectra were obtained on a JEOL ECA, 400 MHz FT NMR Spectrometer or a JEOL ECA, 500 MHz FT NMR Spectrometer. Chemical shifts are reported in ppm on the δ scale relative to TMS as internal standard or to the solvent signal used. Coupling constants are given in Hz. ^{1}H NMR titration experiments were performed on a Bruker Ultrashield ™ 400 PLUS NMR spectrometer. Mass Spectra were obtained on a Finnigan AQA single quadrupole instrument. Chromatographic evaluation of MIPs and non-Imprinted Polymers (NIPs) was performed on an Agilent 1100 series HPLC, using empty chromatography columns (Restek, 50mmX4.6mmX1/4"OD) packed with **MIP1** or **NIP1**. Analysis of equilibrium rebinding experiment samples was performed using a reverse phase column (Kinetex® 5µm C18 100 Å, LC Column 150 x 4.6 mm).

*2.2 Synthesis of Hamilton cleft monomer (**1**)*

2.2.1 *1,3-bis[[6-amino-2-yl)amido]carbonyl]5- tert-butyl-benzene (**3**)*. 5-tert-butylisophthalic acid (**2**, 3 g, 0.0135 mol) was refluxed with 20 mL of $SOCl_2$ for 4 h. The solvent was then evaporated to give the corresponding diacid chloride, which was dissolved in 20 mL of dry THF and then added dropwise to a solution of 2,6-diaminopyridine (14.73 g, 0.135 mol) and triethylamine (TEA) (3.76 mL, 2.73 g, 0.027 mol) in anhydrous THF (220 mL) at 0°C and under a dinitrogen atmosphere. The reaction mixture was stirred at room temperature overnight. The next day the solvent

was evaporated and the crude product washed with water. The sticky solid was filtered, dissolved in hot ethyl acetate and filtered again. The filtrate was evaporated to give a brown solid, which was then purified via column chromatography using silica gel as the stationary phase and ethyl acetate as the eluent. The first fraction eluted from the column was the desired intermediate **3** (light brown solid, 88%).

^{1}H NMR (400 MHz, DMSO-*d*$_6$): δ 1.372 (s, 9H, tert-butyl-CH_3), 5.796 (s, 4H, NH_2), 6.29 (dd, ^{2}J =0.8 Hz, ^{3}J =8 Hz, 2H, Py-CH_2[H-5]), 7.41 (dd, ^{2}J =0.8 Hz, ^{3}J =8 Hz, 2H, Py-CH_2[H-3]), 7.45 (t, ^{3}J =7.6 Hz, 2H, Py-CH_2[H-4]), 8.11 (d, ^{3}J =1.2 Hz, 2H, Ph-CH-4 and 6), 8.33 (s, 1H, Ph-CH-2), 10.292 (s, 2H, NH) ppm. **^{13}C NMR (400 MHz, DMSO-*d*$_6$)**: δ 31.507 (tert-butyl-CH_3), 35.384 (tert-butyl-C), 102.401 (Py-CH_2[C-5]), 104.642 and 139.565 (Py-CH_2[C-3 and C-4]), 124.86 (Ph-C-2), 128.576 (Ph-C-4 and 6), 134.694, 150.982, 151.945, 159.156, and 165.717 ppm. **MS** [M-H$^+$]: 403.49. **HRMS** (ESI-TOF) m/z: [M+H]$^+$ Calcd for $C_{22}H_{25}N_6O_2H$ 405.46; Found 405.203. **IR**: cm^{-1} 1526.6, 1614.9, 1697.4, 2965.1, 3317.4, 3450.2; **mp:** 99-104^{o}C.

2.2.2. *1,3-bis[[6-bisacrylamid-2-yl)amido]carbonyl]5- tert-butyl-benzene (**1**)*. To a solution of **3** (3.5g, 8.65 mmol) and triethylamine (3.61 mL, 2.62 g, 25.95 mmol) in anhydrous THF (180 mL), 1.75 mL of acryloyl chloride (1.95 g, 21.62 mmol) in 20 mL of THF was added slowly at 0°C and under a dinitrogen atmosphere. The reaction mixture was stirred at room temperature overnight. The next day the precipitate was filtered off and the solvent evaporated. The residue was washed with water and saturated aqueous sodium bicarbonate ($NaHCO_3$). The solid was then sonicated in 100 mL of DCM. **1** was obtained as a white solid in a 52% yield (2.3 g).

^{1}H NMR (400 MHz, DMSO-*d*$_6$): δ 1.41 (s, 9H, tert-butyl-CH_3), 5.80 (dd, ^{2}J = 2 Hz, ^{3}J=12 Hz, 2H, CH_{cis} =), 6.33 (dd, ^{2}J = 1.6 Hz, ^{3}J=20 Hz, 2H, CH_{trans}=), 6.67 (dd, $^{3}J_{cis}$= 10.4 Hz, $^{3}J_{trans}$= 16. Hz, 2H, -CH=), 7.87 (m, ^{3}J =8 Hz, 4H, Py-CH_2[H-3 and H-4]), 7.95(m, ^{3}J =4 Hz, 2H, Py-CH_2[H-5]), 8.21 (d, ^{3}J =1.6 Hz, 2H, Ph-CH-4 and 6), 8.382 (s, 1H, Ph-CH-2), 10.458 (s, 2H, NH-C^6), 10.593 (s, 2H, NH-C^2) ppm. **^{13}C NMR (400 MHz, DMSO-*d*$_6$)**: δ 31.50 (tert-butyl-CH_3), 35.510 (tert-butyl-C), 110.778 (Py-CH_2[C-5]), 111.586 and 140.707 (Py-CH_2[C-3 and C-4]), 125.747 (Ph-C-2), 128.439 (CH_2=), 128.67 (Ph-C-4 and 6), 132.089 (-CH=), 134.655, 150.897, 151.035, 152.060, 164.298 and 166.076 ppm. **MS** [M+H$^+$]: 513. **HRMS** (ESI-TOF) m/z: [M+H]$^+$ Calcd for $C_{28}H_{29}N_6O_4H$ 513.56; Found 513.224. **IR**: cm^{-1} 977.6, 1638.9, 1691.6, 2962, 3277.5; **mp:** 223-229^{o}C.

2.3 NMR titration experiments

2.3.1 Job plot

This was performed to give information on the molar ratio of monomer **1** on interaction with a barbiturate guest in solution. Solutions of host and guest (both 5 mM) were prepared in deuterated chloroform ($CDCl_3$). Then 7 different samples with a molar ratio (x_r) ranging from 1 to 0 were prepared by mixing the respective solutions. A chemical shift (δ) of the amido proton in the functional monomer was determined. The product $x_r \cdot \Delta\delta$ was then plotted against the molar ratio to obtain the Job plot.

2.3.2 Association constant determination

NMR titrations were performed in $CDCl_3$ or CD_3CN at 25°C. To a 0.1 or 1 mM monomer solution was added an increasing amount of guest. The complexation induced shift of various protons in the host was determined and then plotted against the concentration of free guest. The produced curves were non-linearly fitted to the 1:1 binding isotherm, described by equation 1, using *OriginPro 8.5.1*

$$\Delta\delta = \frac{K_a [Guest]_{free}}{1+K_a [Guest]_{free}} \cdot \Delta\delta_{max}$$

where K_a (M^{-1}) refers to the binding strength between the monomer and the template. $\Delta\delta_{max}$ is the maximum chemical shift calculated which refers to the plateau of the binding curve, when the host monomer is totally complexed with the guest.

2.4 Polymer synthesis

The imprinted polymer (**MIP1**) was prepared using a molar ratio of *template/functional monomer/cross-linker* of 1:1:20, ABDV as the initiator and chloroform as the solvent/porogen. The control, non-imprinted polymer (**NIP1**) was prepared in an identical fashion but in the absence of the template; acetic acid was used to solubilise the functional monomer. The amounts of reagents used are shown in Table 1.

The template, functional monomer, cross-linking monomer and ABDV (1% w/w total monomers) were dissolved in chloroform ($CHCl_3$) and then introduced to a borosilicate polymerisation tube. The solution was cooled on ice and degassed for 10 min with dinitrogen in order to remove dissolved oxygen. The tube was then sealed using a

flame. The polymerisation was initiated by placing the sealed tubes in a water bath set at 50°C. Polymerisation was allowed to continue for a period of 24 hours at this temperature, after which the tubes were removed from the water bath, broken with a hammer and the monolithic polymers recovered. The resulting monoliths were lightly crushed to give smaller particles, which were then extracted with methanol using a Soxhlet apparatus over a period of 24 hours to remove the template (and unreacted species) from the polymeric matrix and reveal the imprinted binding cavities.

The methanol extracts were evaporated to dryness and weighed; they were then analysed by ^{1}H NMR to identify the composition of the extract. The washed polymer particles were then crushed and sieved, with and the size fraction 25-50 µm collected for further use. These particles were then subjected to sedimentation in methanol to remove fine particles prior to further use. For both polymers, particles of the desired size were obtained in a yield of *ca.* 50%.

Name	***Function***	***mmol***	***MIP1***	***NIP1***
1	functional monomer	1	513 mg	513 mg
Pentobarbital	template	1	226 mg	-
Acetic acid	solubilising agent			0.672 mL
EGDMA	crosslinker	20	3.77 mL (3.96 g)	3.77 mL (3.96 g)
(ABDV)	initiator	1% w/w monomers	52 mg	52 mg
Chloroform	solvent/porogen		5.6 mL	5.6 mL

Table 1: Pre-polymerisation formulations of **MIP1** and **NIP1**.

2.5. Equilibrium batch rebinding experiments

Equilibrium binding experiments were performed on the MIPs and NIPs to evaluate the affinity of the polymers towards the template. The saturation capacity and association constant for the binding sites are obtained by means of these experiments. To 10 mg of polymer particles (25–50 µm, 10 mg dry weight) was added 1mL of template solution in acetonitrile or 1% acetic acid/acetonitrile (v/v) at different concentrations (0 – 10 mM) in HPLC vials. The vials were left at room temperature

over a period of 24 hours, after which the supernatant was examined using HPLC with UV detection at different wavelengths depending on the analyte in question (typically) 245, 260 and 275nm, to obtain the concentration of free template in the supernatant in each vial. The experimental data were fitted to the mono-Langmuir model, using the Origin Pro 8.5.1 software, to obtain an adsorption isotherm and calculate number of sites and related binding constants. The Langmuir model was chosen as it provided the best fit to the binding isotherm data obtained ($R^2 > 0.98$).

2.6 Evaluation of polymer performance by high performance liquid chromatography

The polymers were evaluated by HPLC in order to determine the retention factor on the imprinted polymers of the template used, template analogues, related and non-related compounds (Figure 1). MIP and NIP particles (25–50 µm, 200 mg dry weight) were slurry packed under gravity into separate stainless steel HPLC columns (50 mm x 4.6 mm), using an acetonitrile suspension of particles. The columns were then connected to the HPLC and acetonitrile was continuously passed through the column at a flow rate of 5 mL/min until the signal from injection of acetone (void volume marker) was acceptable (sharp and symmetrical peak).

Before starting the analysis, each column was washed with 1% v/v acetic acid/acetonitrile to ensure the polymers were template free, and then washed again with acetonitrile or the eluent used for the analysis. Prior to analysis, 5mM stock solutions of the analytes were prepared in deionised water or acetonitrile and diluted in water or acetonitrile to give 1 mM solutions. HPLC analyses were performed by injecting 5 µL of these 1 mM analyte solutions at 25 °C, using a flow rate of 1 mL/min. The elution profiles were recorded at different wavelengths (245, 260 and 275nm) depending on the analytes under study. The retention factors (k') for each analyte were calculated as $k' = (t_R-t_0)/t_0$, where t_0 is the retention time of the void marker (acetone) and t_R is the retention time of the analyte. Imprinting factors (IF) were calculated using the formula IF = k' (MIP) / k' (NIP). The selectivity (α) of the polymers were calculated as $\alpha(\text{pentobarbital}) = k_{\text{pentobarbital}}' / k_z'$ where “z” a structurally related analyte.

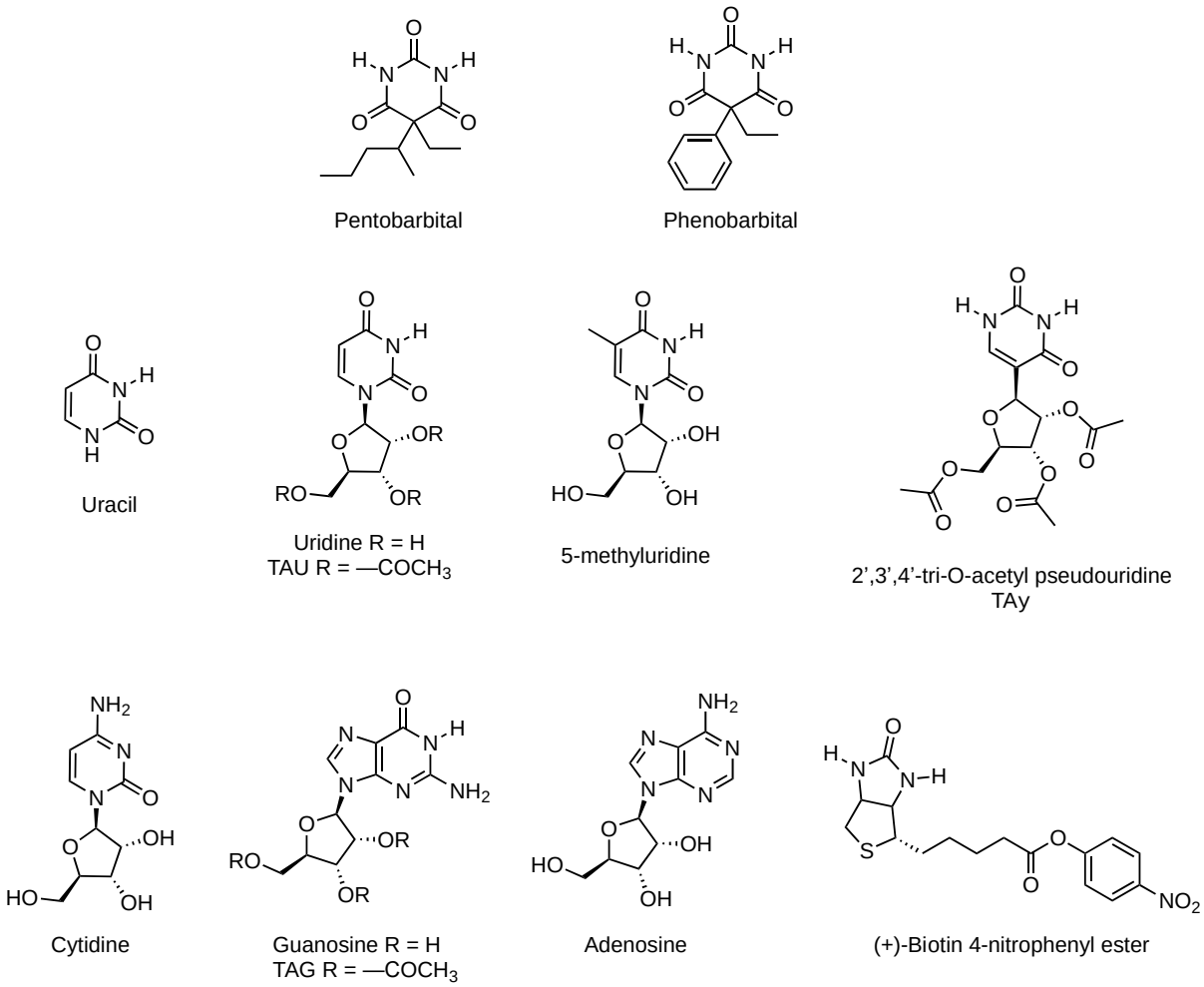

Figure 1: Structures of template molecule and analytes used in the chromatographic evaluation of the polymers.

2.7 Molecular modelling studies

Initial structures of the Hamilton cleft monomer **1** and pentobarbital were constructed in ChemOffice and geometry optimised using molecular mechanics. Additional conformations of the Hamilton cleft were generated using the Frog2 algorithm [33]. From those generated an additional six conformers, each relatively low in energy, were selected to explore the differing binding as the cleft structure changes (Figure S3). Each cleft and barbiturate structure was energy minimised using Gaussian09 [34] using the 6-31G** basis set and the B3LYP functional. Once optimised the barbiturate was introduced to the cleft and the bound complex re-optimised. The binding energy is calculated as the difference between the energy of the bound system and the isolated cleft and barbiturate.

3. Results and discussion

3.1. Monomer synthesis

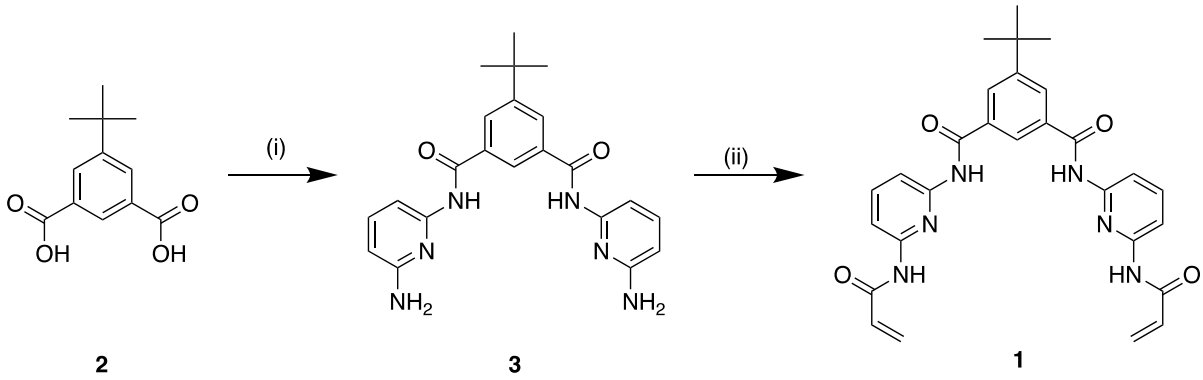

Figure 2: Synthesis of novel functional monomer **1**. Conditions: (i) (a) $SOCl_2$, reflux; (b) 2,6-diaminopyridine, triethylamine, THF (anh), 0ºC to rt; (ii) acryloyl chloride, triethylamine, THF (anh), 0ºC to rt.

The design of the cleft-style monomer **1** was based on the acyclic barbiturate receptors reported by Hamilton *et al.* [29, 30]. The two-step synthesis, depicted in Figure 2, proceeded smoothly to yield the monomer as a white solid in 46% overall yield. Analytical data confirmed the success of the synthesis. The 5-*tert*-butyl group on the isophthaloyl spacer unit was chosen to impart enhanced solubility to the monomer structure.

3.2. NMR titrations

The 1:1 stoichiometry of the interaction between **1** and the barbiturates pentobarbital and phenobarbital was determined via Job plot analysis (Supplementary Information Figure S1). The same stoichiometry was confirmed with the related molecules TAU and TAψ. Further titration experiments were then performed to determine the strength of the interaction between the monomer and the respective guests, with the results presented in Table 2.

1 interacts very strongly with both barbiturate analytes in chloroform solution, with apparent association constants of *ca.* 8 x 10^5 M^{-1}. It should be noted that this is close to the cut-off for determination of association constants using NMR, but the results confirm that the monomer and potential templates for MIP preparation bind strongly in a stoichiometric manner. This ensures that complex formation prior to MIP preparation is assured. On changing the solvent to CD_3CN, the strength of the interaction of **1** with

phenobarbital falls by three orders of magnitude, indicating the effect of the more polar solvent environment.

GUEST	***K_a (M^{-1})***	***$\Delta\delta_{max}$***	***[M1] (mM)***	***solvent***
Pentobarbital	80536 ± 8%	1.63 ± 0.01	0.1	$CDCl_3$
Phenobarbital	88602 ± 12%	1.66 ± 0.01	0.1	$CDCl_3$
2',3',4'-tri-O-acetyluridine (TAU)	1288 ± 2%	1.58 ± 0.01	1	$CDCl_3$
2',3',4'-tri-O-acetyl pseudouridine (TAψ)	117 ± 8%	1.87 ± 0.09	1	$CDCl_3$
Ethylene urea	12 ± 19%	6.55 ± 1.18	1	$CDCl_3$
Phenobarbital	80 ± 7.5%	1.63 ± 0.01	1	CD_3CN

Table 2: Association constants (K_a (M^{-1})) for the complexation of **1** with various guests). $\Delta\delta_{max}$ is the maximum change in the chemical shift. Values were calculated by fitting the experimental data to a 1:1 binding isotherm using OriginPro 8.5.1.

While the other guests are able to form complexes with **1**, they form fewer hydrogen bonds with the cleft structure and so exhibit much lower association constants than do the two barbiturate guests.

3.3 Polymer preparation

The synthesis of the pentobarbital-imprinted and control, non-imprinted polymers proceeded smoothly. Each polymerisation was conducted over 24 hours at 50ºC using ABDV as the initiator. The white monolithic polymers obtained were extracted using methanol in a Soxhlet apparatus for 24 hours, after which they were crushed and sized to give particles in the desired 25 – 50 μm size range in *ca.* 50% yield.

The extracts from each polymer were evaporated to dryness and analysed by gravimetry and by ^{1}H NMR, to confirm the quantity extracted and the identity of compounds contained in the extracts (Supplementary Information Figure S2). The MIP and NIP extracts had masses of 280 mg and 2 mg, respectively. The ^{1}H NMR spectra of the extracts shows the clear presence of the template pentobarbital, together with oligomeric material, in the MIP extract, while the NIP shows only oligomeric material.

IR analysis of the extracted polymers show the identical chemical composition of the polymers, with the MIP spectrum showing no evidence of the pentobarbital template. The amount of pentobarbital used in the MIP formulation was 228 mg. Taking the gravimetric, NMR and IR analyses together implies that all template has been removed from the MIP, leaving the imprinted binding sites free to rebind the template and related analytes. From the masses of the respective extracts, assuming 100% template removal from the MIP, suggests that the amount of oligomeric material extracted from the MIP is much greater than that extracted from the NIP (a difference of 54 mg). This suggests that the presence of the template has affected the rate of polymerisation in the case of the MIP *vis-à-vis* the NIP. The effect of the template on the rate of MIP polymerisation has been rarely reported formally, though anecdotal evidence suggests that it is a commonplace. A reported example is the work of McCluskey *et al.* [35] who attempted to prepare imprinted thin films for the recognition of 2,4-dinitrotoluene and 2,4,6-trinitrotoluene, which are known chain-transfer agents. They found that that the molecular weights of the polymers prepared decreased as the concentration of the nitroaromatic templates increased. While the template effect in this case is not stark, it is worthy of mention.

3.4 Equilibrium rebinding experiments

These experiments were performed on **MIP1** and **NIP1** to evaluate the affinity of the polymers towards the template molecule. The binding isotherms for each polymer are presented in Figure 3. It is evident that **MIP1** has far greater affinity for pentobarbital than does **NIP1**. The experimental data were most suitably fitted using the Langmuir model and the results are shown in Table 3.

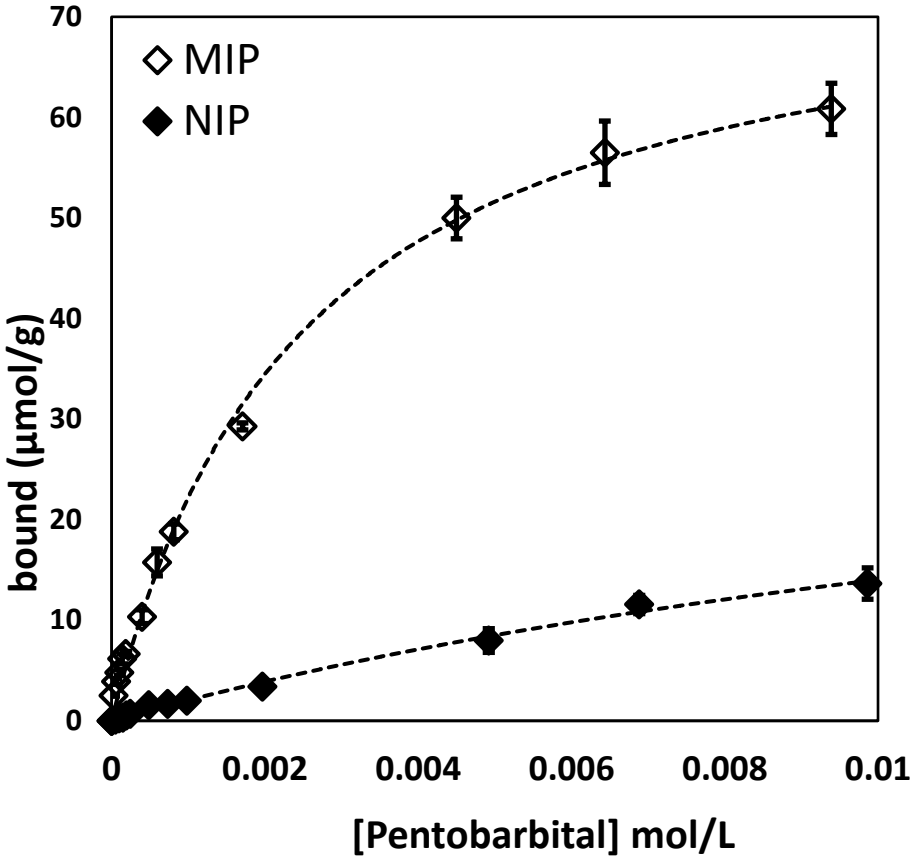

Figure 3: *Binding isotherms obtained with equilibrium rebinding experiments of **MIP1** and **NIP1** in acetonitrile. Pentobarbital concentration = 0-10mM. All experiments were repeated in triplicate. The [pentobarbital]$_{free}$ in the supernatant was evaluated with HPLC (wavelength: 240 nm, Flow rate: 1 m L/ min, Injection: 5µL, RSD % < 21, n = 3).*

	K_a	N (µmol/g)	R^2
MIP1	403.23	77	0.99557
NIP1	54.08	40	0.9943

Table 3: *Binding constants (K_a) and number of sites (N) of **MIP1** and **NIP1**.*

The marked differences in affinity can be explained through the imprinting process, which appears to have created a reasonably high population of binding sites with high affinity in the case of **MIP1**. In contrast, the absence of the template in the preparation of **NIP1** has led to a lower population of binding sites with lower affinity.

3.5 Chromatographic evaluation

We further assessed the recognition capabilities of **MIP1** and **NIP1** in chromatographic experiments, using each polymer as the stationary phase. Along with the template, a range of related analytes were used to determine the selectivity of the polymers. Initial experiments using acetonitrile as mobile phase were unsuccessful in eluting the template molecule from **MIP1** within a 60-minute timeframe, indicating strong retention. After experimentation with additives (acetic acid and TFA), we chose a mobile phase of 1%TFA in acetonitrile. While template elution was still not possible, the use of a more acidic eluent would have led to instrument damage. The results of the chromatographic evaluation are shown in Table 4.

The retention behaviour of the template on **NIP1** is in stark contrast to its retention behaviour on **MIP1**, with rapid elution of the template observed on the non-imprinted polymer, leading to an exceptionally high imprinting factor. A similar effect is seen for the related molecule phenobarbital, which was also not eluted from **MIP1**, yet is poorly retained by **NIP1**, demonstrating the cross-selectivity of **MIP1**.

The retention of all other analytes on **MIP1** is comparatively low. Those analytes bearing a stronger structural resemblance to the template, i.e. uracil, uridine and 5-methyluridine, were better retained by **MIP1** than the structurally unrelated analytes, leading to moderate imprinting factors. These analytes were also more strongly bound to **NIP1** than all other analytes. This suggests that residues of monomer **1** are accessible within NIP1 and able to engage in hydrogen-bonding interactions with analytes containing an ADA array, but that the two ADA “arms” of **1** are unable to act in concert to allow for strong binding to the template or phenobarbital.

Clearly, these differences in retention and recognition of the barbiturate analytes are a result of the imprinting process rather than the inherent affinity of monomer **1** itself to the different analytes. The elution behaviour of the two barbiturates *vis-à-vis* the other analytes indicates that **MIP1** could be used in solid phase extraction protocols, where there is less limitation on the choice of elution solvent.

Analyte	Parameter	MIP1	NIP1
Pentobarbital	k' ±SD[a] α (pentobarbital) IF	>**90.84** ± 0.00 1.0 >**199.72**	0.45 ± 0.01 1.0
Phenobarbital	k' ±SD[a] α (pentobarbital) IF	>**90.84** ± 0.00 1.0 >**160.55**	0.57 ± 0.01 0.8
Biotin-NO2	k' ±SD[a] α (pentobarbital) IF	0.19 ± 0.00 468.5 1.34	0.14 ± 0.01 3.1
Uracil	k' ±SD[a] α (pentobarbital) IF	4.90 ± 0.36 18.5 1.94	2.53 ± 0.11 0.2
Uridine	k' ±SD[a] α (pentobarbital) IF	2.06 ± 0.06 44.2 1.69	1.22 ± 0.09 0.4
TAU	k' ±SD[a] α (pentobarbital) IF	0.36 ± 0.03 250.8 2.5	0.24 ± 0.00 4.6
TAψ	k' ±SD[a] α (pentobarbital) IF	0.12 ± 0.01 741.8 1.21	0.10 ± 0.01 4.5
5-MeU	k' ±SD[a] α (pentobarbital) IF	2.43 ± 0.15 37.3 1.61	1.51 ± 0.06 0.3
Adenosine	k' ±SD[a] α (pentobarbital) IF	-0.33 ± 0.03 > 908.4 0.94	-0.35 ± 0.01 > 4.6
Cytidine	k' ±SD[a] α (pentobarbital) IF	-0.36 ± 0.03 > 908.4 1.01	-0.36 ± 0.03 > 4.6
Guanosine	k' ±SD[a] α (pentobarbital) IF	-0.34 ± 0.00 > 908.4 0.96	-0.36 ± 0.02 > 4.6
TAG	k' ±SD[a] α (pentobarbital) IF	-0.42 ± 0.04 > 908.4 1.14	-0.37 ± 0.02 > 4.6

Table 4: *Selectivity and specificity of template/analytes on MIP1 and NIP1 in 1% TFA/acetonitrile (v/v) as mobile phase. Selectivity α(p) = k_p'/k_z'; p = pentobarbital, z = structurally related analyte. For analytes with a negative k', a fixed value of k' = 0.1*

*was used. [a] SD (standard deviation, n=3). RSD [(relative standard deviation) = (SD/x) *100, x= mean value] = 2-11.*

There exists the possibility that the differences in retention behaviour on the analytes on **MIP1** and **NIP1** is due to differences in polymer morphology, given the use of acetic acid as a solubilising agent in the preparation of **NIP1**. However, the very similar retention on each polymer of those analytes not containing an imide-like functionality (adenosine, cytosine, guanosine, TAG) suggests that this is not a large contributor to the effects observed.

3.6 Molecular modelling studies

The results obtained from the chromatographic evaluation of the materials show a marked difference in the behaviours of the imprinted and non-imprinted polymer. We hypothesised that the presence of the template alters the preferred conformation of monomer **1** and that the imprinting process “locks in” this preference. In an attempt to explain these differences, we conducted molecular modelling studies looking at the preferred structures for monomer **1** in the absence and presence of the template molecule.

A selection of the lowest energy conformers of monomer **1** are shown in Figure 4 (for conformers 1-7, see Figure S3), with the lowest energy conformer (Cleft 1) and an “opened cleft” (Cleft 3) shown for clarity in Figure 4 below. We can see how the opening of the cleft by rotation of the “arms” leads to less stable conformers. Whilst we would expect the majority of monomer **1** to present in solution as this most stable structure, we would also expect significant populations of the some of the higher energy structures, particularly conformer 3. We may also expect the structures to be interconverting.

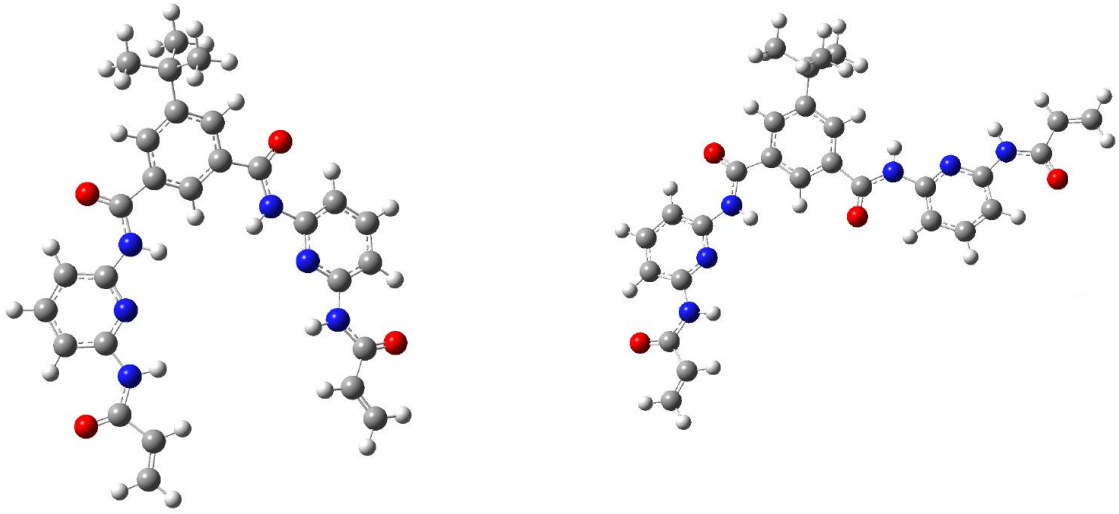

Cleft 1 Cleft 3

Figure 4. Computed **1** structures. Cleft 1 the most stable conformation and Cleft 3 is an illustrative sample of a more open structure – that shown is the 2nd most stable conformation considered.

Likewise, given the relatively small differences in energy, on polymerisation in the absence of the template (**NIP1**), there will be a variety in cleft conformation present. Thus, we may expect that **NIP1**, whilst possessing some regions that maintain the cleft structure, will also comprise less specific binging sites. The impact of the presence of these less specific sites is clear from the binding energy we compute for the isolated molecule – a NIP comprising regions such as cleft 7 is not likely to bind the pentobarbital very strongly, as we see experimentally.

Cleft Structure	**Relative Energy of Cleft (kJ mol^{-1})**	**Binding energy with pentobarbital (kJ mol^{-1})**
1	0.0	-123.5
3	26.2	-80.0
2	52.5	-110.8
6	78.8	-37.2
5	105.0	-36.9
7	131.3	-81.2
4	183.7	-48.2

Table 5. Computed relative energies and pentobarbital binding strength of a sample of monomer 1 conformers. Structures are shown in Figure S3. Labelling refers to energy ranking in Frog2. Relative energy and binding energy computed using DFT.

The MIP is formed from a solution where the monomer is pre-bound to the pentobarbital. Hence the high binding energy of the pentobarbital to the most stable conformer will increase considerably the population of these conformers in solution. Furthermore, the high binding energy means this cleft conformation is more "locked" by the presence of the template. We therefore suggest that the resulting polymer will also have more of the cleft in this strongly binding geometry in its structure and, hence, be more specific for pentobarbital, as found experimentally.

Thus by exerting a templating effect, the template "chooses" the conformer of the monomer unit to be locked in place during MIP synthesis, which in turn leads to recognition properties showing higher specificity and selectivity.

4. Conclusions

In this paper, we have demonstrated the benefits of using a designed functional monomer in the stoichiometric imprinting of barbiturates. The monomer, based on the Hamilton cleft, is readily accessible and delivers outstanding recognition capabilities. The MIP prepared from this monomer shows a high degree of specificity and selectivity for barbiturates. This is likely derived from the effect of the template during both the pre-polymerisation complexation, where it "chooses" the most appropriate conformer of the monomer, and during the polymerisation, where we speculate that the cross-linking nature of the monomer assists in "locking in" the preferred monomer conformation within the polymer structure. This "locking in" effect is likely to be important in the design of larger and more complex functional monomers, e.g. aptamers, and we believe that such monomers will likely require more than one anchor point in the growing imprinted polymer chains to operate effectively, i.e. the monomer should act as both a recognition unit *and* as a crosslinking agent. In this work we have assessed the binding properties of **MIP1** using organic media in both dynamic and equilibrium conditions. Any real-life application of **MIP1** will require the use of aqueous media and future work will examine its behaviour of the materials under such conditions. To this end, we are currently studying the potential of **MIP1** in solid phase extraction protocols for the clean-up and enrichment of barbiturates from biological samples.

5. Acknowledgements

SL would like to thank the University of Kent for a Doctoral Studentship.

6. References

[1] F. López-Muñoz, R. Ucha-Udabe, C. Alamo, The history of barbiturates a century after their clinical introduction. Neuropsychiatr. Dis. Treat. 1 (2005) 329-343.

[2] J. Skibiski, S. Abdijadid, Barbiturates. [Updated 2020 Nov 20]. In: StatPearls [Internet]. Treasure Island (FL): StatPearls Publishing; 2021 Jan-. Available from: https://www.ncbi.nlm.nih.gov/books/NBK539731/

[3] M. J. Brodie, P. Kwan, Current position of phenobarbital in epilepsy and its future. Epilepsia. 53 (2012) Suppl 8:40-6. doi: 10.1111/epi.12027.

[4] J. Wood, C. Ferguson, Best evidence topic report. Procedural sedation for cardioversion. Emerg. Med. J. 23 (2006) 932-934. doi: 10.1136/emj.2006.043067.

[5] E. John, A. Butt, Deaths related to drug poisoning in England and Wales: 2019 registrations. Office for National Statistics, U.K Government, 14 October 2020. Available from: https://www.ons.gov.uk/releases/deathsrelatedtodrugpoisoninginenglandandwales2019registrations

[6] L. Ye, K. Mosbach, Molecular imprinting: synthetic materials as substitutes for biological antibodies and receptors. Chem. Mater. 20 (2008) 859-868. doi: 10.1021/cm703190w.

[7] G. Vlatakis, L. I. Andersson, R. Müller, K. Mosbach, Drug assay using antibody mimics made by molecular imprinting. Nature. 361 (1993) 645-647. doi: 10.1038/361645a0.

[8] F. G. Tamayo, J. L. Casillas, A. Martin-Esteban, Clean-up of phenylurea herbicides in plant sample extracts using molecularly imprinted polymers. Anal. Bioanal. Chem. 381 (2005) 1234-1240. doi: 10.1007/s00216-005-3071-1.

[9] Y. Hoshino, T. Kodama, Y. Okahata, K. J. Shea, Peptide imprinted polymer nanoparticles: a plastic antibody. J. Am. Chem. Soc. 130 (2008) 15242-15243. doi: 10.1021/ja8062875.

[10] R. Mahajan, M. Rouhi, S. Shinde, T. Bedwell, A. Incel, L. Mavliutova, S. Piletsky, I. A. Nicholls, B. Sellergren, Highly Efficient Synthesis and Assay of Protein-Imprinted Nanogels by Using Magnetic Templates. Angew Chem .Int. Ed. Engl. 58 (2019) 727-730. doi: 10.1002/anie.201805772.

[11] G. Jamalipour Soufi, S. Iravani, R. S. Sharma, Molecularly imprinted polymers for the detection of viruses: Challenges and opportunities. Analyst 146 (2021) 3087-3100. doi: 10.1039/d1an00149c.

[12] S. Piletsky, F. Canfarotta, A. Poma, A. M. Bossi, S. Piletsky, Molecularly Imprinted Polymers for Cell Recognition. Trends Biotechnol. 38 (2020) 368-387. doi: 10.1016/j.tibtech.2019.10.002.

[13] E. Turiel, A. Martin-Estaban, Molecularly imprinted polymers-based microextraction techniques. TrAC 118 (2019) 574-586. 10.1016/j.trac.2019.06.016

[14] A. Yarman, S. Kurbanoglu, I. Zebger, F. W. Scheller, Simple and robust: The claims of protein sensing by molecularly imprinted polymers. Sensor. Actuat. B-Chem. 330 (2021) Article number 129369. 10.1016/j.snb.2020.129369

[15] K. Haupt, P. X. Medina Rangel, B. T. S. Bui, Molecularly Imprinted Polymers: Antibody Mimics for Bioimaging and Therapy. Chem. Rev. 120 (2020) 9554-9582. doi: 10.1021/acs.chemrev.0c00428.

[16] S. Xu, L. Wang, Z. Liu, Molecularly Imprinted Polymer Nanoparticles: An Emerging Versatile Platform for Cancer Therapy. Angew. Chem. Int. Ed. Engl. 60 (2021) 3858-3869. doi: 10.1002/anie.202005309.

[17] J. Q. Liu, G. Wulff, Functional mimicry of carboxypeptidase A by a combination of transition state stabilization and a defined orientation of catalytic moieties in molecularly imprinted polymers. J. Am. Chem. Soc. 130 (2008) 8044-8054. doi: 10.1021/ja8012648.

[18] S. Nestora, F. Merlier, S. Beyazit, E. Prost, L. Duma, B. Baril, A. Greaves, K. Haupt, Plastic antibodies for cosmetics: Molecularly imprinted polymers scavenge precursors of malodors. Angew. Chem. Int. Ed. 55 (2016), 6252-6256. doi: 10.1002/anie.201602076.

[19] A. J. Hall, P. Manesiotis, M. Emgenbroich, M. Quaglia, E. De Lorenzi, B. Sellergren, Urea host monomers for stoichiometric molecular imprinting of oxyanions. J. Org. Chem. 70 (2005) 1732-1736. doi: 10.1021/jo048470p.

[20] J. Chen, S. Shinde, M.-H. Koch, M. Eisenacher, S. Galozzi, T. Lerari, K. Barkovits, P. Subedi, R. Kruger, K. Kuhlmann, B. Sellergren, S. Helling, Low-bias phosphopeptide enrichment from scarce samples using plastic antibodies. Sci. Rep. 5 (2015), article number 11438. Doi: 10.1038/srep11438.

[21] P. X. Medina Rangel, E. Moroni, F. Merlier, L. A. Gheber, R. Vago, B. T. S. Bui, K. Haupt, Chemical antibody mimics inhibit cadherin-mediated cell-cell adhesion: A promising strategy for cancer therapy. Angew. Chem. Int. Ed. Engl. 59 (2020) 2816-2822. doi: 10.1002/anie.201910373.

[22] A. Poma, H. Brahmbhatt, H. M. Pendergraff, J. K. Watts, N. W. Turner, Generation of novel hybrid aptamer-molecularly imprinted polymeric nanoparticles. Adv. Mater. 27 (2015) 750-758. doi: 10.1002/adma.201404235.

[23] Q. Li, S. Shinde, G. Grasso, A. Caroli, R. Abouhany, M. Lanzillotta, G. Pan, W. Wan, K. Rurack, B. Sellergren, Selective detection of phospholipids using molecularly imprinted fluorescent sensory shell particles. Sci. Rep. 10 (2020), article number 9924. doi: 10.1038/s41598-020-66802-3.

[24] D.T. Seidenkranz, M. D. Pluth, Fluorescent Arylethynyl Hamilton Receptors for Barbiturate Sensing. J. Org. Chem. 84 (2019) 8571-8577. doi: 10.1021/acs.joc.9b00978.

[25] G. A. Shabir, T. K. Bradshaw, S. A. Arain, G. Q. Shar, A New Validated Method for the Simultaneous Determination of a Series of Eight Barbiturates by RP-HPLC. J. Liq. Chromatogr. Relat. Technol. 33 (2010), 61-71. doi: 10.1080/10826070903430175.

[26] Y. Hoshino, H. Koide, T. Urakami, H. Kanazawa, T. Kodama, N. Oku, K. J. Shea, Recognition, Neutralization, and Clearance of Target Peptides in the Bloodstream of Living Mice by Molecularly Imprinted Polymer Nanoparticles: A Plastic Antibody. J. Am. Chem. Soc. 132 (2010) 6644-6645. doi: 10.1021/ja102148f.

[27] K. Tanabe, T. Takeuchi, J. Matsui, K. Ikebukuro, K. Yano, I. Karube, Recognition of barbiturates in molecularly imprinted copolymers using multiple

hydrogen bonding. J. Chem. Soc., Chem. Commun. (1995) 2303-2304; doi: 10.1039/C39950002303

[28] H. Kubo, H. Nariai, T. Takeuchi, Multiple hydrogen bonding-based fluorescent imprinted polymers for cyclobarbital prepared with 2,6-bis(acrylamido)pyridine. Chem. Commun. 3 (2003) 2792-2793. doi: 10.1039/b309917b

[29] S.-K. Chang, A. D. Hamilton, Molecular recognition of biologically interesting substrates: synthesis of an artificial receptor for barbiturates employing six hydrogen bonds. J. Am. Chem. Soc. 110 (1988), 1318-1319. doi: 10.1021/ja00212a065.

[30] E. Fan, A. D. Hamilton, S.-K. Chang, D. Van Engen, Hydrogen bonding and molecular recognition: synthetic, complexation, and structural studies on barbiturate binding to an artificial receptor. J. Am. Chem. Soc. 113 (1991) 7640-7645. doi: 10.1021/ja00020a027.

[31] A. Winqvis, R. Stromberg, Investigation on Condensing Agents for Phosphinate Ester Formation with Nucleoside 5'-Hydroxyl Functions, Eur. J. Org. Chem. (2008) 1705-1714. doi: 10.1002/ejoc.200700528

[32] A. Krstulja, S. Lettieri, A. J. Hall, R. Delépée, P. Favetta, L. A. Agrofoglio, Evaluation of molecularly imprinted polymers using 2',3',5'-tri-O-acyluridines as templates for pyrimidine nucleoside recognition. Anal. Bioanal. Chem. 406 (2014) 6275-6284. doi: 10.1007/s00216-014-8017-z.

[33] M. Miteva, F. Guyon, P. Tuffery, Frog2: Efficient 3D conformation ensemble generator for small compounds. Nucleic Acids Res. 38 (2010) W622-7. doi: 10.1093/nar/gkq325

[34] M. J. Frisch, G. W. Trucks, H. B. Schlegel, G. E. Scuseria, M. A. Robb, J. R. Cheeseman, G. Scalmani, V. Barone, G. A. Petersson, H. Nakatsuji, X. Li, M. Caricato, A. Marenich, J. Bloino, B. G. Janesko, R. Gomperts, B. Mennucci, H. P. Hratchian, J. V. Ortiz, A. F. Izmaylov, J. L. Sonnenberg, D. Williams-Young, F. Ding, F. Lipparini, F. Egidi, J. Goings, B. Peng, A. Petrone, T. Henderson, D. Ranasinghe, V. G. Zakrzewski, J. Gao, N. Rega, G. Zheng, W. Liang, M. Hada, M. Ehara, K. Toyota, R. Fukuda, J. Hasegawa, M. Ishida, T. Nakajima, Y. Honda, O. Kitao, H. Nakai, T. Vreven, K. Throssell, J. A. Montgomery, Jr., J. E. Peralta, F. Ogliaro, M. Bearpark, J. J. Heyd, E. Brothers, K. N. Kudin, V. N. Staroverov, T. Keith, R. Kobayashi, J. Normand, K. Raghavachari, A. Rendell, J. C. Burant, S. S. Iyengar, J. Tomasi, M. Cossi, J. M. Millam, M. Klene, C. Adamo, R. Cammi, J. W. Ochterski, R. L. Martin, K. Morokuma, O. Farkas, J. B. Foresman, and D. J. Fox, Gaussian, Inc., Wallingford CT, 2016.

[35] N. W. Turner, N. Holmes, C. Brisbane, A. B. McGeachie, M. C. Bowyer, A. McCluskey, C. I. Holdsworth, Effect of template on the formation of phase-inversed molecularly imprinted polymer thin films: An assessment. Soft Matter 5 (2009), 3663-3671. doi: 10.1039/b902468a.

Supplementary Information

Figure S1. Job Plot for monomer **1** with pentobarbital, phenobarbital, TAU and TAψ. The monomer interacts with the analytes in a 1:1 stoichiometric complex. The experiments were made in $CDCl_3$ using 5mM monomer and template concentration solution. X_r = molar fraction Δδ = chemical shift change.

Figure S2. ^1H NMR spectra for methanolic extracts from (i) **MIP1** and (ii) **NIP1**. Dried extracts were dissolved in DMSO-d_6.

Figure S3. Structures of all the monomer **1** conformers considered in the computational study.

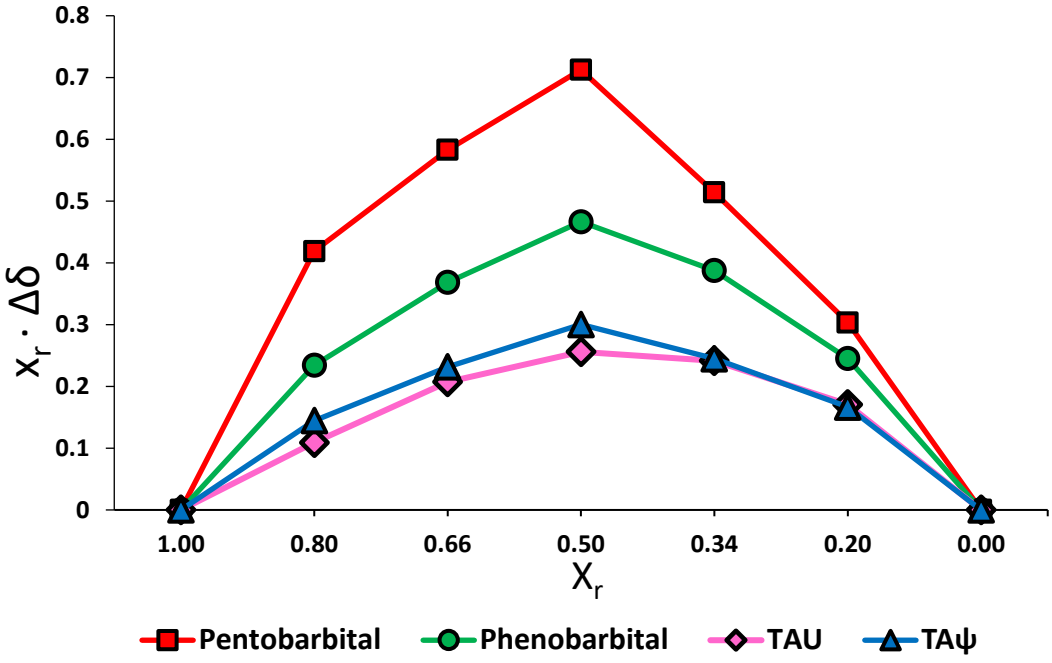

Figure S1. Job Plot for monomer **1** with pentobarbital, phenobarbital, TAU and TAψ. The monomer interacts with the analytes in a 1:1 stoichiometric complex. The experiments were made in $CDCl_3$ using 5mM monomer and template concentration solution. X_r = molar fraction Δδ = chemical shift change.

(i) MIP extract (total mass = 288 mg)

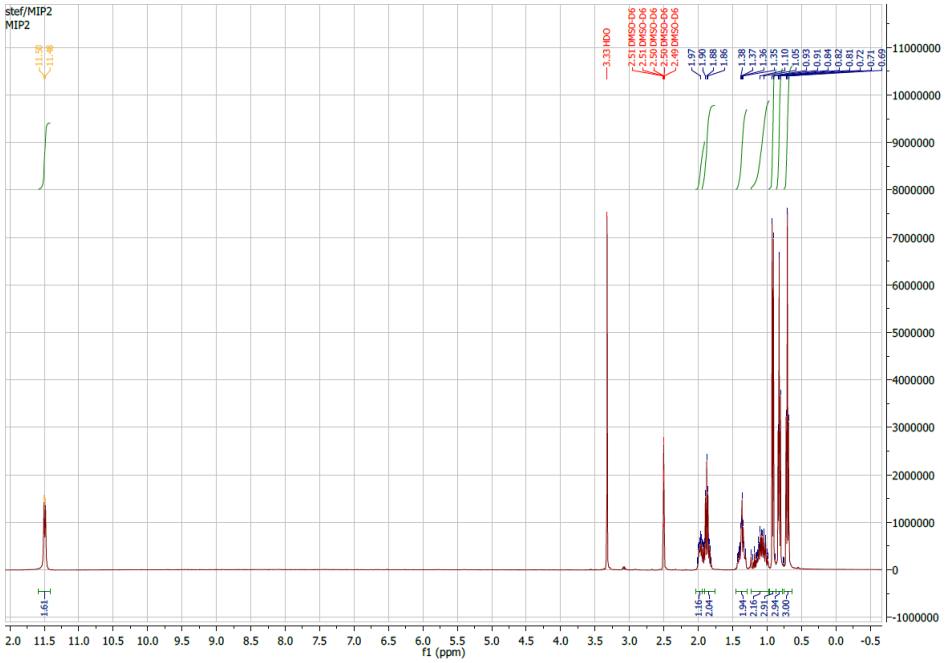

(ii) NIP extract (total mass = 2 mg)

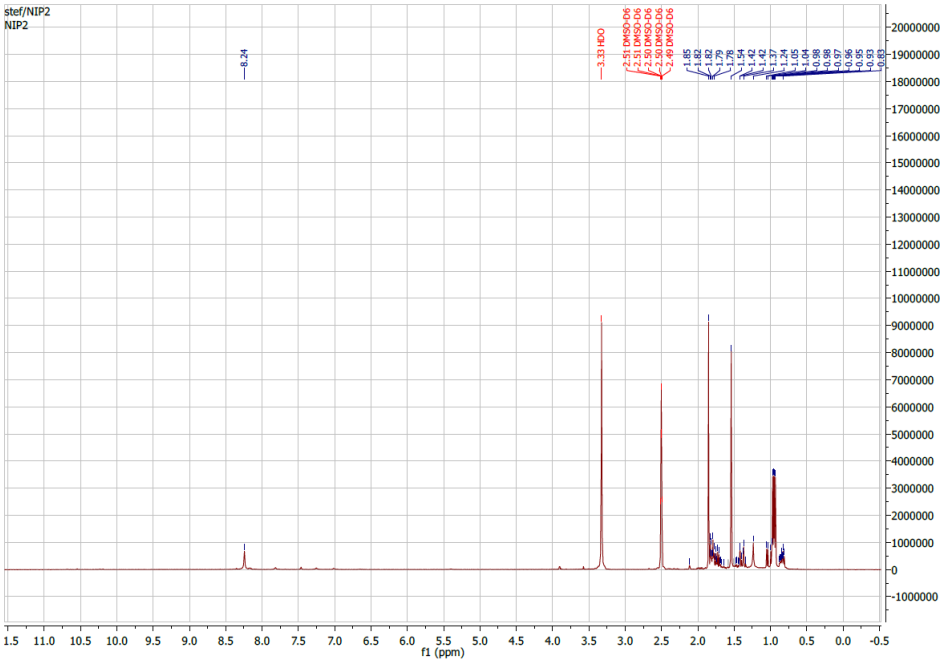

Figure S2. ^{1}H NMR spectra for methanolic extracts from (i) **MIP1** and (ii) **NIP1**. Dried extracts were dissolved in DMSO-d_6.

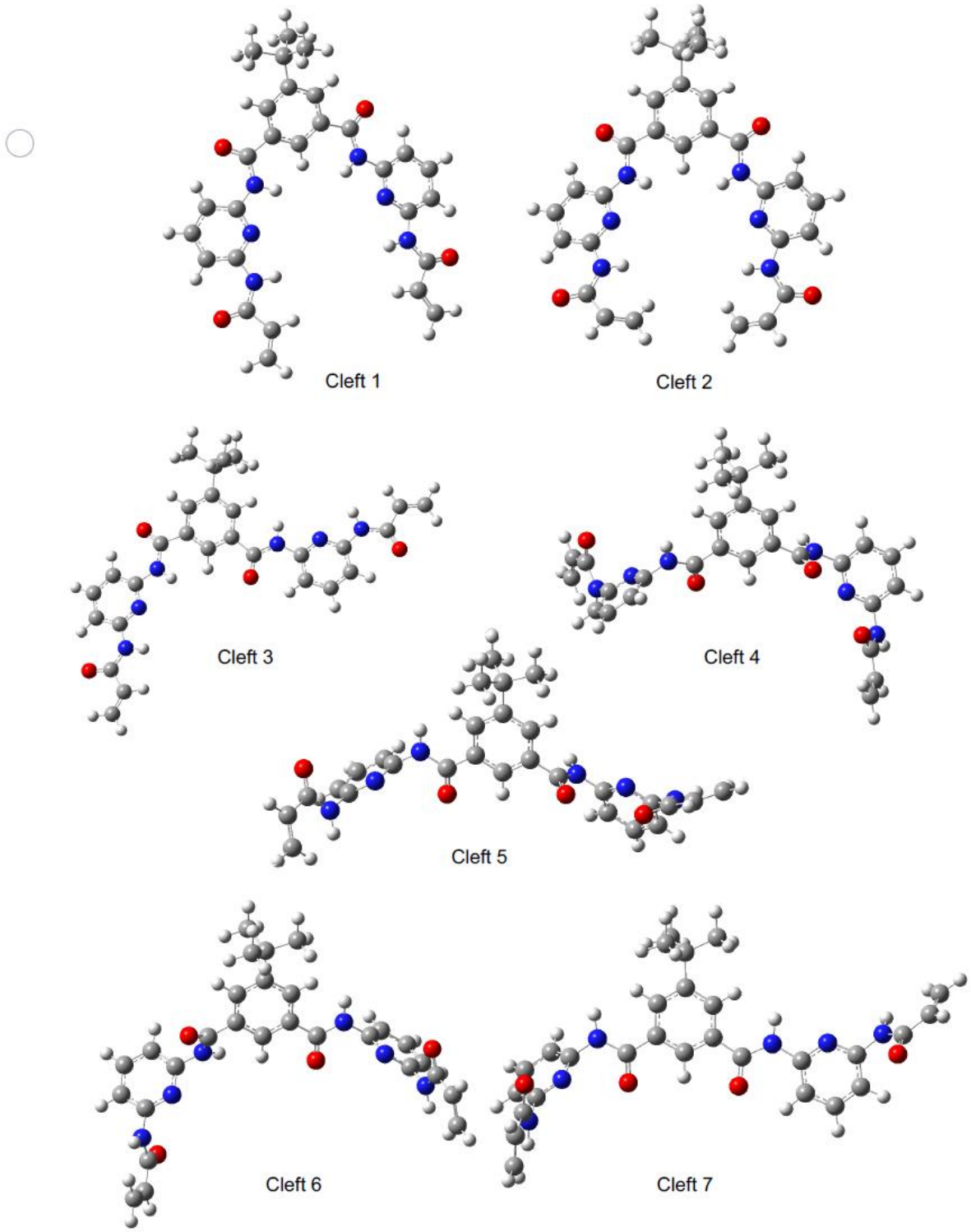

Figure S3. Structures of all the monomer **1** conformers considered in the computational study.